Accepted Manuscript

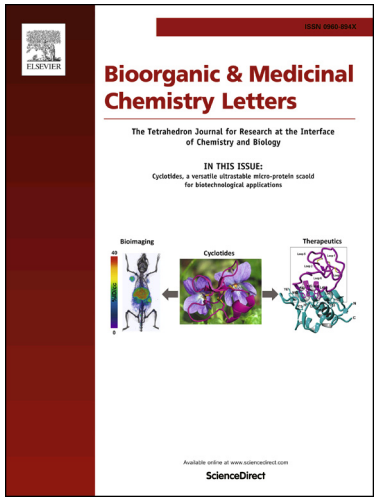

Factors affecting the uncaging efficiency of 500 nm light-activatable BODIPY caging group

Minoru Kawatani, Mako Kamiya, Hironori Takahashi, Yasuteru Urano

PII: S0960-894X(17)31117-4
DOI: https://doi.org/10.1016/j.bmcl.2017.11.030
Reference: BMCL 25436

To appear in: *Bioorganic & Medicinal Chemistry Letters*

Received Date: 2 October 2017
Accepted Date: 15 November 2017

Please cite this article as: Kawatani, M., Kamiya, M., Takahashi, H., Urano, Y., Factors affecting the uncaging efficiency of 500 nm light-activatable BODIPY caging group, *Bioorganic & Medicinal Chemistry Letters* (2017), doi: https://doi.org/10.1016/j.bmcl.2017.11.030

Graphical Abstract

To create your abstract, type over the instructions in the template box below.
Fonts or abstract dimensions should not be changed or altered.

Factors affecting the uncaging efficiency of 500 nm light-activatable BODIPY caging group

Leave this area blank for abstract info.

Minoru Kawatani, Mako Kamiya, Hironori Takahashi and Yasuteru Urano

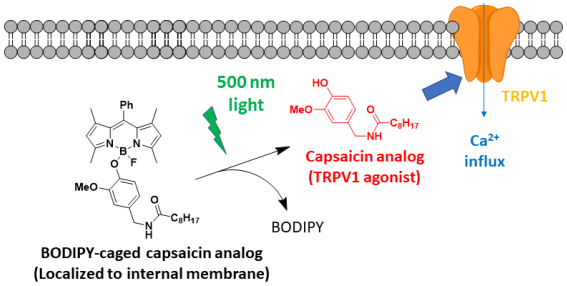

Bioorganic & Medicinal Chemistry Letters
journal homepage: www.elsevier.com

Factors affecting the uncaging efficiency of 500 nm light-activatable BODIPY caging group

Minoru Kawatani[a], Mako Kamiya[ab], Hironori Takahashi[a] and Yasuteru Urano[acd, *]

[a]*Graduate School of Medicine, The University of Tokyo7-3-1 Hongo, Bunkyo-ku, Tokyo, 113-0033, Japan*
[b]*PRESTO, Japan Science and Technology Agency, 4-1-8 Honcho, Kawaguchi, Saitama, 332-0012, Japan*
[c]*Graduate School of Pharmaceutical Sciences, The University of Tokyo7-3-1 Hongo, Bunkyo-ku, Tokyo, 113-0033, Japan*
[d]*CREST, Japan Agency for Medicinal Research and Development, 1-7-1 Otemachi, Chiyoda-ku, Tokyo, 100-0004, Japan*

ARTICLE INFO

Article history:
Received
Revised
Accepted
Available online

Keywords:
Caged compound
BODIPY
Photo-induced electron transfer (PeT)
Capsaicin
TRPV1

ABSTRACT

Photoremovable protective groups, or caging groups, enable us to regulate the activities of bioactive molecules in living cells upon photoirradiation. Nevertheless, requirement of UV light for activating caging group is a significant limitation due to its cell toxicity and its poor tissue penetration. Our group previously reported a 500 nm light-activatable caging group based on BODIPY scaffold, however, its uncaging efficiency was lower than those of conventional caging groups. Here we show that the uncaging quantum yield (QY) of BODIPY caging group depends upon the driving force of photo-induced electron transfer (PeT). We also found that the uncaging QY increased in less polar solvents. We applied these findings to develop BODIPY-caged capsaicin, which is well localized to low-polarity intracellular compartments, as a tool to stimulate TRPV1 in live cells in response to blue-green light.

* Corresponding author. Tel.: +81-03-5841-3601; fax: +81-03-5841-3563; e-mail: uranokun@m.u-tokyo.ac.jp

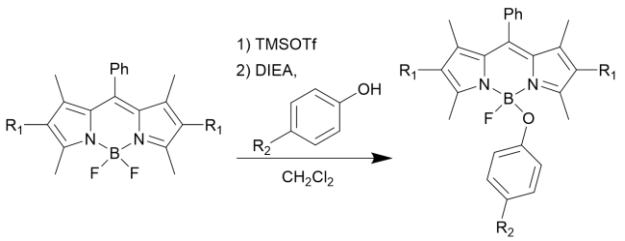

Photoremovable protective groups, also referred to as caging groups, are widely used in biological research to manipulate the activity of molecules of interest in a spatiotemporally controlled manner[1,2]. Various caging groups have been developed, but in most cases the uncaging reaction requires ultraviolet (UV) to cyan light (250-400 nm), which is harmful to living cells and has limited tissue penetration[3,4]. Although multi-photon excitation with red to near-infrared light avoids this problem, simultaneous activation of a wide field of view is still challenging[5].

To achieve one-photon excitation with longer-wavelength light (> 500 nm), several caging groups have been developed. For example, the structures of conventional caging groups such as *o*-nitrobenzyl or coumarin have been extensively evolved, but their maximum excitation wavelengths are still under 500 nm[6,7]. Amine-ruthenium complex can be excited by light over 500 nm, but may cause photodamage to living cells due to its photosensitivity[8]. Other types of biocompatible caging groups have been developed based on boron dipyrromethene (BODIPY)[9–12], cyanine[13], or cobalamin[14], with excitation wavelengths over 500 nm. Our group reported 4-aryloxy BODIPY derivatives that undergo single-photon uncaging reaction with 500 nm light for releasing phenols (Scheme 1)[11]. The BODIPY caging group has several favourable properties for biological applications, such as a long excitation wavelength, a sharp absorption spectrum, traceability of its localization by the intrinsic fluorescence of BODIPY, and the high extinction coefficient of BODIPY scaffold. However, in that work, we found that the uncaging quantum yield (QY) ($\phi_u < 1\times10^{-3}$) was much smaller than that of conventional UV light-activatable caging groups, resulting in reduced uncaging efficiency, which is determined by the product of ε and ϕ_u ($\varepsilon\phi_u$).

Here, aiming to improve this situation, we examined the factors that affect the uncaging QY of the BODPY caging group. In our previous report, 4-aryloxy BODIPY derivatives, whose fluorescence was well quenched through photo-induced electron transfer (PeT), showed higher uncaging QY than derivatives whose fluorescence was not quenched[11]. Thus, we hypothesized that the charge separation state generated by PeT would be the key intermediate to trigger deprotection. Therefore, we first examined whether optimization of the PeT process would maximize the uncaging QY of the BODIPY caging group.

For this purpose, we prepared a series of BODIPY derivatives with different PeT efficiencies. According to our previous report, the HOMO energy level (oxidation potential) of an aryl group (electron donor) and the LUMO energy level (reduction potential) of a fluorophore (electron acceptor) are major determinants of PeT efficiency[15,16]. Therefore, we designed and synthesized 16 4-aryloxy BODIPY derivatives, which have different combinations of aryl groups (electron donor) and BODIPY cores (electron acceptor) (Scheme 2). DFT calculations revealed that introduction of electron-withdrawing or donating substituents at the 2,6-positions of the BODIPY core (R_1) or the *para*-position of the aryl group (R_2) effectively altered the HOMO / LUMO energy levels, respectively (Table S1).

We then examined the spectroscopic and photochemical properties of the synthesized derivatives in methanol (Table 1, Fig. S1, Table S2, Table S3). Substituents on aryl groups had little effect on the maximum absorption and emission wavelengths, whereas introduction of an ethyl or a chloride group onto the BODIPY core induced a red shift of about 25 nm in the absorption and emission spectra compared with non-substituted analogues. As expected, fluorescence QYs (ϕ_{fl}) were decreased as the HOMO energy level of the aryl group increased (R_2: COOMe < CH_2COOMe < Me < OMe) and as the LUMO energy levels of the BODIPY core declined (R_1: Et > H > Cl > COOAM).

To evaluate whether fluorescence QYs and uncaging QYs were dependent on PeT efficiency, we calculated the PeT efficiency (driving force of PeT) of each derivative. According to the Rehm-Weller equation (equation 1)[17], the driving force of PeT can be calculated as the change in free energy (ΔG_{PeT}).

$$\Delta G_{PeT} = E_{ox} - E_{red} - E_{00} - w \quad \text{(eq. 1)}$$

where E_{ox} and E_{red} represent oxidation potential (HOMO energy level) of the donor and reduction potential (LUMO energy level) of the acceptor, respectively. E_{00} is the singlet excitation energy of the fluorophore. The work term for the charge separation state w is considered as constant due to the structural similarity between the synthesized BODIPY derivatives. Therefore, we used the sum of ΔG_{PeT} and w [$\Delta G_{PeT} + w$] as an index of the driving force of PeT, and fluorescence QYs or uncaging QYs were plotted against this index value (Fig. 1). As a

Table 1 Spectroscopic and photochemical properties of 4-phenoxy BODIPY derivatives in methanol.[a]

R_1	R_2		λ_{abs} [nm]	ϕ_{fl}	ϕ_u [$\times10^{-4}$]
Et	COOMe	**(1)**	523	0.62	N. D.[c]
	CH_2COOMe	**(2)**	523	0.42	19.8 ± 0.4
	Me	**(3)**	523	0.15	51.8 ± 2.1
	OMe	**(4)**	522	0.013	19.2 ± 0.4
H	COOMe	**(5)**	499	0.52	2.8 ± 0.2
	CH_2COOMe	**(6)**	498	0.035	44.6 ± 3.6
	Me	**(7)**	498	0.029	53.8 ± 2.2
	OMe	**(8)**	500	0.011	25.6 ± 0.1
Cl	COOMe	**(9)**	524	0.32	6.5 ± 0.2
	CH_2COOMe	**(10)**	522	0.038	19.3 ± 0.1
	Me	**(11)**	524	0.060	23.0 ± 3.3
	OMe	**(12)**	525	0.004	7.6 ± 1.6
COOAM[b]	COOMe	**(13)**	495	0.038	14 ± 1.4
	CH_2COOMe	**(14)**	496	0.003	12.7 ± 0.9
	Me	**(15)**	495	0.024	12.8 ± 0.4
	OMe	**(16)**	496	0.002	6.9 ± 0.3

a λ_{abs}: maximum absorption wavelength, ϕ_{fl}: fluorescence quantum yield, ϕ_u: uncaging quantum yield, Uncaging QY was determined from the degradation of 4-phenoxy BODIPY derivatives. Data are presented as mean ± SEM from three independent experiments. b AM: acetoxymethyl (-CH_2OCOCH_3), c N.D.: not determined due to the low uncaging efficiency.

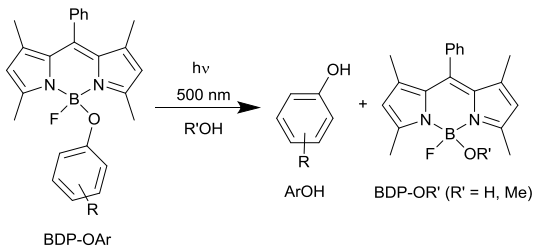

Scheme 1 General scheme of the uncaging of 4-aryloxy BODIPY derivatives[11].

result, it was found that fluorescence QYs tend to decrease as the driving force of PeT increases. In contrast, the relationship between uncaging QYs and the driving force of PeT showed a different pattern. In the range where [$\Delta G_{PeT} + w$] was higher than 0.035 hartree, fluorescence quenching by PeT was not sufficient, and uncaging QY tended to be suppressed. Similarly, where [$\Delta G_{PeT} + w$] was lower than 0.025 hartree, uncaging QY decreased again, possibly due to the increasing rate of back electron transfer from the charge-separated intermediate, a pathway competing with the uncaging reaction. On the other hand, the derivatives showing [$\Delta G_{PeT} + w$] of around 0.03 hartree tended to show relatively high uncaging QY. Furthermore, when the highest uncaging QYs in each BODIPY core ((**3**), (**7**), (**11**) and (**13**)) were compared, the derivatives whose R_1 substituents are Et (**3**) and H (**7**) showed higher values than those of Cl (**11**) and COOAM (**13**). The highest uncaging QY among the 16 derivatives was observed when R_1 = H and R_2 = Me (**7**) (ϕ_u = 0.54%), which was 2.1 times higher than that of our previously reported derivative (R_1 = H and R_2 = OMe (**8**)).

Next, we evaluated the effect of solvent polarity on uncaging QY. Solvent polarity affects the efficiency of PeT, changing the threshold of fluorescence quenching[16], but little is known about the effect on uncaging efficiency. We selected (**7**), which showed the highest uncaging QY in methanol, and examined the fluorescence and uncaging QY in five different solvents; dimethylsulfoxide (DMSO, dielectric constant[18]; ε_r = 48.9), acetonitrile (CH_3CN, ε_r = 37.5), dichloromethane (CH_2Cl_2, ε_r = 9.1), toluene (ε_r = 2.3), and hexane (ε_r = 1.9) (Fig. 2, Fig. S2, Table S4, Table S5). As previously reported, fluorescence QY was increased in less polar solvents. Interestingly, uncaging QYs also increased in less polar solvents. Similar tendencies were observed with other derivatives ((**6**) and (**8**)) (Fig. S3). We observed that the uncaging efficiency ($\varepsilon\phi_u$) of (**7**) in hexane reached 1.4 x 10^3 $M^{-1}cm^{-1}$, which is the highest, to our knowledge, so far reported among the longer-wavelength (> 500 nm) activatable caging groups.

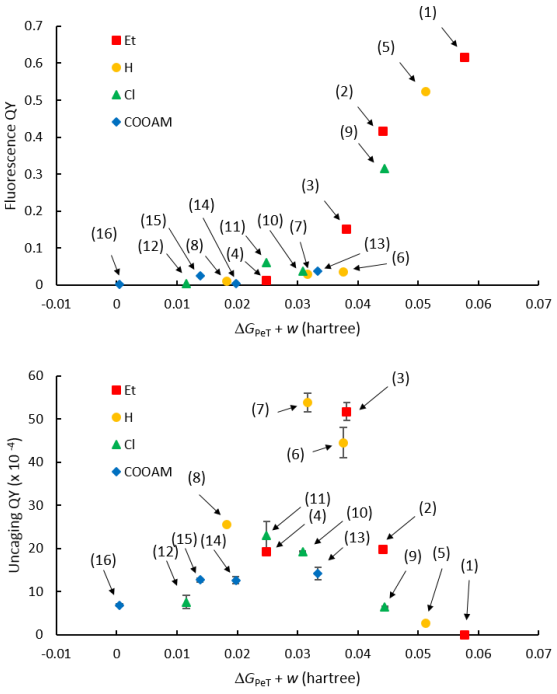

Fig. 1 Fluorescence (above) and uncaging (bottom) QY of each compound was plotted against the driving force of PeT (ΔG_{PeT} + w). Red, orange, green, and blue colour indicates the substituent on the BODIPY core (R_1).

Considering that BODIPY derivatives are known to be localized to internal cell membranes, such as endoplasmic reticulum (ER), Golgi apparatus, and mitochondria, where the polarity is considered to be much lower than that of water[11,16], we expected that a sufficiently high uncaging efficiency could be attained with our BODIPY caged molecule in living cells.

In order to confirm the usefulness of our findings and the utility of BODIPY as a caging scaffold to release a bioactive molecule at internal membranes in living cells, we newly designed and synthesized BODIPY-caged capsaicin, BDP-CAP (Fig. 3a), consisting of a BODIPY core and a capsaicin analogue, pelargonic acid vanillylamide (PAVA), which is an agonist of transient receptor potential cation channel V1 (TRPV1)[19–22]

PAVA was chosen since its binding site on TRPV1 is at an intracellular location, and thus, intracellularly uncaged PAVA should bind effectively to TRPV1 and would be expected to perturb the cell function efficiently. Moreover, protection of the

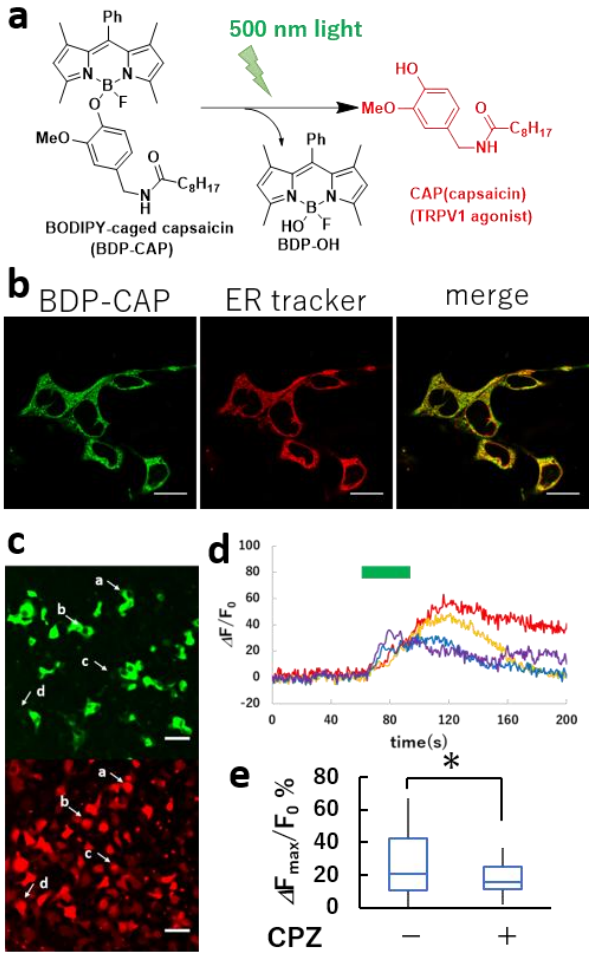

Fig. 3 (a) Photoreaction scheme of BDP-CAP. (b) Intracellular localizations of BDP-CAP (green) and ER tracker (red), also colocalization of the two (yellow region). Scale bar, 20 μm. (c) Expression patterns of TRPV1-GFP (green) and staining patterns of CaTM3 (red) in HEK293 cells. Scale bar, 50 μm. (d) Representative traces of intracellular Ca^{2+} dynamics upon green light illumination (green bar). Each line colour corresponds to a different cell: cell a (red), b (yellow), c (blue), and d (purple) indicated in figure 2(c). Cells a and b represented high-TRPV1-expressing cells, while cells c and d represented low-TRPV1-expressing cells. (e) Statistical analysis of Ca^{2+} dynamics upon green light illumination with and without 10 μM capsazepine (CPZ). Mean ± SEM, *p < 0.001, Student's t-test, n = 40 cells from two independent experiments.

phenol moiety of capsaicin derivatives has been reported to block their biological activity[19,22–25].

Further, we selected hydrogen as a substituent on the BODIPY core (R_1) to optimize PeT efficiency, as the calculated HOMO energy level of PAVA was between those of *p*-cresol and *p*-methoxyphenol (-0.211 hartree, Table S1). *In vitro* characterization of BDP-CAP revealed that the uncaging quantum yield of BDP-CAP consumption in methanol (ϕ_u = 0.21 ± 0.03%) was similar to that of the derivative (**8**), and the uncaging efficiency ($\varepsilon^*\phi_u$ = 134 ± 19 $M^{-1}cm^{-1}$) should be sufficient for light-triggered TRPV1 activation in living cells[22]. Moreover, BDP-CAP was well colocalized with ER marker in HEK 293 cells (Fig. 3b). Thus, we expected that uncaging of BDP-CAP would proceed efficiently in living cells.

Encouraged by these results, we next applied BDP-CAP to HEK293 cells that had been transiently transfected with TRPV1 (Fig. 3c). Since TRPV1 stimulation with PAVA induces calcium influx, changes in intracellular Ca^{2+} concentration were monitored with the red calcium sensor, CaTM3[26]. When 2 μM BDP-CAP was loaded into the cells, no clear calcium signal was observed (Fig. S4). But, upon light stimulation with a blue-green argon laser on a standard laser-scanning microscope, a rapid increase of CaTM3 fluorescence was detected (Fig. 3d). This calcium influx was effectively inhibited in the presence of 10 μM capsazepin (CPZ), a selective TRPV1 antagonist (Fig. 3e). Taken together, these results support the idea that BODIPY-caged compounds localized to internal membrane can efficiently release bioactive molecules to stimulate cell physiology in response to 500 nm light illumination.

In summary, we uncovered the relationship between the driving force of PeT and uncaging QY of the BODIPY caging group, and found that a suitable substituent on the BODIPY core was effective to improve the uncaging QY. Moreover, the solvent dependency of uncaging efficiency indicated that low polarity also improves the uncaging QY. This is favourable for intracellular uncaging of a bioactive molecule, because BODIPY derivatives generally localize at the intracellular membrane. Based on these findings, we designed and synthesized a photo-activatable TRPV1 channel agonist, BDP-CAP. Although the chemical yield of PAVA production was limited to 28 ± 2% (Table S6), the caged compound effectively stimulated TRPV1-expressing HEK293 cells only when the cells were exposed to visible uncaging light. Recent research has revealed that exclusive intra- or extracellular localization of a bioactive molecule is crucial for signaling outcome[27]. Thus, we believe that BODIPY caging groups would serve as a useful caging scaffold for intracellular uncaging applications. Finally, our findings should also be helpful to develop red-shifted BODIPY caging groups that would be useful for *in vivo* application.

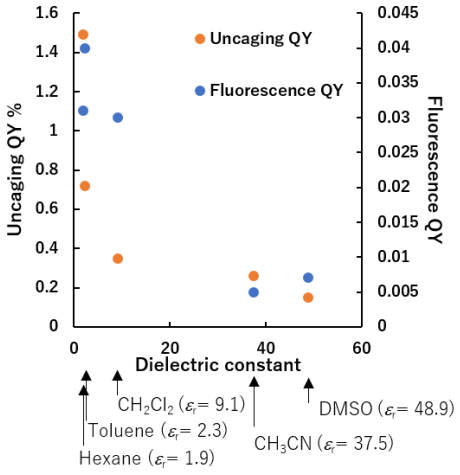

Fig. 2 Uncaging and fluorescence quantum yield of (**7**) in various solvents. ε_r: dielectric constant, Uncaging QY was determined from the degradation of 4-phenoxy BODIPY derivatives.

Acknowledgments

This research was supported in part by AMED/CREST, by JST/PRESTO (JPMJPR14F8), by MEXT/JSPS KAKENHI Grant Numbers JP16H02606 (to Y.U.), JP26111012 (Y.U.), JP15H05951 "Resonance Bio" (to M.K.), by JSPS Core-to-Core Program, by a grant from Hoansha Foundation (to Y.U.), and by stipend from the Graduate Program for Leaders in Life Innovation (GPLLI) to M.K. CaTM3-AM was a kind gift from Dr. K. Hanaoka.

Supplementary Material

Supplementary data associated with this article can be found, in the online version, at XXX.

References and notes

1. Ellis-davies, G. C. R. *Nat. Methods* **2007**, *4*, 619–628.
2. Mayer, G.; Hechel, A. *Angew. Chemie Int. Ed.* **2006**, *45*, 4900–4921.
3. Kla, P.; Bochet, C. G.; Givens, R.; Rubina, M.; Popik, V.; Kostikov, A.; Wirz, J. *Chem. Rev.* **2013**, *113*, 119–191.
4. Brieke, C.; Rohrbach, F.; Gottschalk, A.; Mayer, G.; Heckel, A. *Angew. Chemie Int. Ed.* **2012**, *51*, 8446–8476.
5. Matsuzaki, M.; Hayama, T.; Kasai, H.; Ellis-Davies, G. C. R. *Nat. Chem. Biol.* **2010**, *6*, 255–7.
6. Agarwal, H. K.; Janicek, R.; Chi, S.-H.; Perry, J. W.; Niggli, E.; Ellis-Davies, G. C. R. *J. Am. Chem. Soc.* **2016**, *138*, 3687–3693.
7. Olson, J. P.; Banghart, M. R.; Sabatini, B. L.; Ellis-Davies, G. C. R. *J. Am. Chem. Soc.* **2013**, *135*, 15948–15954.
8. DeRosa, M. C.; Crutchley, R. J. *Coord. Chem. Rev.* **2002**, *233–234*, 351–371.
9. Rubinstein, N.; Liu, P.; Miller, E. W.; Weinstain, R. *Chem. Commun.* **2015**, *51*, 6369–6372.
10. Goswami, P. P.; Syed, A.; Beck, C. L.; Albright, T. R.; Mahoney, K. M.; Unash, R.; Smith, E. a; Winter, A. H. *J. Am. Chem. Soc.* **2015**, *137*, 3783–3786.
11. Umeda, N.; Takahashi, H.; Kamiya, M.; Ueno, T.; Komatsu, T.; Terai, T.; Hanaoka, K.; Nagano, T.; Urano, Y. *ACS Chem. Biol.* **2014**, *9*, 2242–2246.
12. Takeda, A.; Komatsu, T.; Nomura, H.; Naka, M.; Matsuki, N.; Ikegaya, Y.; Terai, T.; Ueno, T.; Hanaoka, K.; Nagano, T.; Urano, Y. *ChemBioChem* **2016**, *17*, 1233–1240.
13. Gorka, A. P.; Nani, R. R.; Zhu, J.; Mackem, S.; Schnermann, M. J. *J. Am. Chem. Soc.* **2014**, *136*, 14153–14159.
14. Shell, T. a; Shell, J. R.; Rodgers, Z. L.; Lawrence, D. S. *Angew. Chemie Int. Ed.* **2014**, *53*, 875–8.
15. Hattori, S.; Ohkubo, K.; Urano, Y.; Sunahara, H.; Nagano, T.; Wada, Y.; Tkachenko, N. V.; Lemmetyinen, H.; Fukuzumi, S. *J. Phys. Chem. B* **2005**, *109*, 15368–15375.
16. Sunahara, H.; Urano, Y.; Kojima, H.; Nagano, T. *J. Am. Chem. Soc.* **2007**, *129*, 5597–5604.
17. Rehm, D.; Weller, A. *Isr. J. Chem.* **1970**, *8*, 259–271.
18. Dean, J. A. *Langre's Handbook of Chemistry*; **1992**.
19. Walpole, C. S.; Wrigglesworth, R.; Bevan, S.; Campbell, E. A.; Dray, A.; James, I. F.; Masdin, K. J.; Perkins, M. N.; Winter, J. *J. Med. Chem.* **1993**, *36*, 2362–2372.
20. Walpole, C. S.; Wrigglesworth, R.; Bevan, S.; Campbell, E. A.; Dray, A.; James, I. F.; Masdin, K. J.; Perkins, M. N.; Winter, J. *J. Med. Chem.* **1993**, *36*, 2373–2380.
21. Walpole, C. S. J.; Wrigglesworth, R.; Bevan, S.; Campbell, E. A.; Dray, A.; James, I. F.; Masdin, K. J.; Perkins, M. N.; Winter, J. *J. Med. Chem.* **1993**, *36*, 2381–2389.
22. Zhao, J.; Gover, T. D.; Muralidharan, S.; Auston, D. A.; Weinreich, D.; Kao, J. P. Y. *Biochemistry* **2006**, *45*, 4915–4926.

23. Van Ryssen, M. P.; Avlonitis, N.; Giniatullin, R.; McDougall, C.; Carr, J. L.; Stanton-Humphreys, M. N.; Borgström, E. L. a; Brown, C. T. a; Fayuk, D.; Surin, A.; Niittykoski, M.; Khiroug, L.; Conway, S. J. *Org. Biomol. Chem.* **2009**, *7*, 4695–4707.
24. Zemelman, B. V.; Nesnas, N.; Lee, G. A.; Miesenbock, G. *Proc. Natl. Acad. Sci.* **2003**, *100*, 1352–1357.
25. Gilbert, D.; Funk, K.; Dekowski, B.; Lechler, R.; Keller, S.; Möhrlen, F.; Frings, S.; Hagen, V. *ChemBioChem* **2007**, *8*, 89–97.
26. Hirabayashi, K.; Hanaoka, K.; Egawa, T.; Kobayashi, C.; Takahashi, S.; Komatsu, T.; Ueno, T.; Terai, T.; Ikegaya, Y.; Nagano, T.; Urano, Y. *Cell Calcium* **2016**, *60*, 256–265.
27. Nadler, A.; Yushchenko, D. A.; Müller, R.; Stein, F.; Feng, S.; Mulle, C.; Carta, M.; Schultz, C. *Nat. Commun.* **2015**, *6*, 10056.
1.